Journal of Orthopaedic Translation 39 (2023) 147–162

Contents lists available at ScienceDirect

Journal of Orthopaedic Translation

journal homepage: www.journals.elsevier.com/journal-of-orthopaedic-translation

Original Article

Forkhead box O3 attenuates osteoarthritis by suppressing ferroptosis through inactivation of NF-κB/MAPK signaling

Chen Zhao [a,1], Guantong Sun [a,1], Yaxin Li [b,1], Keyu Kong [a], Xiaodong Li [a], Tianyou Kan [a], Fei Yang [a,**], Lei Wang [a,***], Xiaoqing Wang [a,*]

[a] Department of Orthopedics, Shanghai Key Laboratory of Orthopedic Implant, Shanghai Ninth People's Hospital, Shanghai Jiao Tong University School of Medicine, Shanghai, 200011, China

[b] Department of Oral & Cranio-Maxillofacial Surgery, Shanghai Ninth People's Hospital, Shanghai Jiao Tong University School of Medicine, Shanghai, 200011, China

ARTICLE INFO

Keywords:
Osteoarthritis
Ferroptosis
Chondrocyte
Forkhead box O3
Extracellular matrix

ABSTRACT

Background: Ferroptosis is a nonapoptotic cell death process that is characterized by lipid peroxidation and intracellular iron accumulation. As osteoarthritis (OA) progresses, inflammation or iron overload induces ferroptosis of chondrocytes. However, the genes that play a vital role in this process are still poorly studied.

Methods: Ferroptosis was elicited in the ATDC5 chondrocyte cell line and primary chondrocytes by administration of the proinflammatory cytokines, interleukin (IL)-1β and tumor necrosis factor (TNF)-α, which play key roles in OA. The effect of FOXO3 expression on apoptosis, extracellular matrix (ECM) metabolism, and ferroptosis in ATDC5 cells and primary chondrocytes was verified by western blot, Immunohistochemistry (IMHC), immunofluorescence (IF) and measuring Malondialdehyde (MDA) and Glutathione (GSH) levels. The signal cascades that modulated FOXO3-mediated ferroptosis were identified by using chemical agonists/antagonists and lentivirus. In vivo experiments were performed following destabilization of medial meniscus surgery on 8-week-old C57BL/6 mice and included micro-computed tomography measurements.

Results: In vitro administration of IL-1β and TNF-α, to ATDC5 cells or primary chondrocytes induced ferroptosis. In addition, the ferroptosis agonist, erastin, and the ferroptosis inhibitor, ferrostatin-1, downregulated or upregulated the protein expression of forkhead box O3 (FOXO3), respectively. This, suggested, for the first time, that FOXO3 may regulate ferroptosis in articular cartilage. Our results further suggested that FOXO3 regulated ECM metabolism via the ferroptosis mechanism in ATDC5 cells and primary chondrocytes. Moreover, a role for the NF-κB/mitogen-activated protein kinase (MAPK) signaling cascade in regulating FOXO3 and ferroptosis was demonstrated. In vivo experiments confirmed the rescue effect of intra-articular injection of a FOXO3-overexpressing lentivirus against erastin-aggravated OA.

Conclusions: The results of our study show that the activation of ferroptosis promotes chondrocyte death and disrupts the ECM both in vivo and in vitro. In addition, FOXO3 can reduce OA progression by inhibiting ferroptosis through the NF-κB/MAPK signaling pathway.

The Translational potential of this article: This study highlights the important role of chondrocyte ferroptosis regulated by FOXO3 through the NF-κB/MAPK signaling in the progression of OA. The inhibition of chondrocyte ferroptosis by activating FOXO3 is expected to be a new target for the treatment of OA.

Abbreviations: DMM, destabilization of the medial meniscus; ECM, extracellular matrix; Fer-1, ferrostatin-1; FOXO3, forkhead box O3; GSH, glutathione; GPX4, glutathione peroxidase 4; H&E, hematoxylin and eosin; IF, immunofluorescence; IHC, immunohistochemistry; IL-1β, interleukin 1β; MAPK, mitogen-activated protein kinase; OA, osteoarthritis; OARSI, Osteoarthritis Research Society International; RIPA, radioimmunoprecipitation assay; ROS, reactive oxygen species.

* Corresponding author. 639 Zhizaoju Road, Shanghai, 200011, PR China.

** Corresponding author. 639 Zhizaoju Road, Shanghai, 200011, PR China.

*** Corresponding author. 639 Zhizaoju Road, Shanghai, 200011, PR China.

E-mail addresses: feiyangyn@163.com (F. Yang), wanglei12041985@163.com (L. Wang), osteoclast2006@163.com (X. Wang).

[1] These authors contributed equally.

https://doi.org/10.1016/j.jot.2023.02.005

Received 12 October 2022; Received in revised form 3 January 2023; Accepted 20 February 2023

Available online 14 March 2023

1. Introduction

Osteoarthritis (OA) is the most common musculoskeletal disease and is associated with extremely high rates of disability and a reduced quality of life in the older population [1,2]. Currently, there is no effective treatment for OA, except for total knee replacement in patients with advanced OA. Furthermore, the treatment of early OA is mainly limited to relieving pain and reducing joint wear [3–6]. Elucidating the pathogenesis of OA and identifying of new target molecules involved in the pathophysiological process of OA are essential to the prevention and treatment of this disease.

Abnormal death of chondrocytes in the articular cartilage during the development of OA plays an important role in OA progression [7]. Ferroptosis is a nonapoptotic mode of cell death that involves iron-dependent massive lipid peroxidation-mediated membrane damage [8]. Ferroptosis was first reported by Dixon et al. [9] and is inextricably linked to many diseases, including leukemia, pancreatic cancer, liver fibrosis, and OA [10–13].

Recent studies have demonstrated that ferroptosis plays a role in the occurrence and development of OA, and can promote its progression [13]. Although OA and ferroptosis share certain features, such as abnormal iron metabolism [14,15], lipid peroxidation [16,17], and mitochondrial dysfunction [18], research on the genes involved in regulating of OA through the mechanism of ferroptosis is scarce. Because the role of glutathione peroxidase 4 (GPX4), an important marker of ferroptosis, has been sufficiently studied in chondrocytes, the research focus can be shifted to molecular targets with the potential to regulate ferroptosis in OA [10,19–21].

In this study, we determined the upregulation of ferroptosis markers in an IL-1β/TNF-α-driven inflammatory environment, and the role of ferroptosis in the pathological process of OA, using in vitro cells and in vivo animal experiments. The results suggested that forkhead box O3 (FOXO3) was involved in regulating of ferroptosis, that was stimulated by IL-1β and by the ferroptosis agonist, erastin, in OA. Intra-articular injection of a FOXO3-overexpressing lentivirus effectively alleviated the exacerbation of OA caused by a low dose erastin. These findings suggest a mechanism by which FOXO3 regulates ferroptosis resistance and demonstrate the therapeutic potential of ferroptosis-based therapies targeting aberrant chondrocyte death in OA.

2. Materials and methods

2.1. Reagents

A recombinant mouse IL-1β (C600124) and TNF-α (C600052) were purchased from Sangon Biotech (Shanghai, China). Erastin (S7242) and ferrostatin-1 (Fer-1; S7243) were purchased from Selleck (Houston, USA). DCFH-DA (S0033) was purchased from Beyotime (Shanghai, China). The Liperfluo staining reagent (L248) and FerroOrange (F374) were purchased from Dojindo (Shanghai, China).

2.2. Animal experiments

All animal experiments were approved by the Animal Ethics Committee of the Shanghai Ninth People's Hospital. 20 eight-week-old male C57BL/6J mice were purchased from the Shanghai Laboratory Animal Research Center (Shanghai, China) and bred in strict accordance with the rules of laboratory animal feeding. Destabilization of the medial meniscus (DMM) surgery was performed on the right knee joint of 8-week-old male C57BL/6J mice to induce OA by dissecting the medial meniscus ligament [22,23]. The sham group was surgically treated as described above, but without the dissection of the medial meniscal ligament. On the following day, the ferroptosis agonist erastin and/or a FOXO3-encoding lentivirus (1×10^{10} virus particles/10 μL) were injected intra-articularly to test whether FOXO3 overexpression in mouse cartilage tissue preserved cartilage integrity in the erastin-treated OA model (10 μl per joint per mice two times a week for 8 weeks). At week 8, the mice were euthanized, and the joints were collected for histological assessment (n = 5 per group).

2.3. Micro-CT analysis

Before decalcification of knee specimens, high-resolution micro-CT scanning of the low extremities was performed using a Scanco μCT80 system (Scanco Medical, Brüttisellen, Switzerland).

2.4. Histological staining

Lower limb samples were embedded in paraffin and sectioned (5-μm thickness). For histological assessment, the paraffin-embedded tissue sections were stained with safranin O-fast green and hematoxylin and eosin (H&E), in accordance with the manufacturer's instructions (Servicebio). The Osteoarthritis Research Society International (OARSI) score was based on safranin O-fast green staining in each specimen [24].

2.5. Immunohistochemistry (IHC) and immunofluorescence (IF)

Mouse cartilage tissue sections were fixed in 10% formalin for 7 days. After fixation, formalin-fixed specimens were embedded in paraffin. IHC or IF staining was performed with antibodies against GPX4 (Abcam, ab125066; dilution 1:100), collagen II (Abcam, ab34712; dilution 1:100), and FOXO3 (Cell Signaling Technology, D19A7; dilution 1:100).

2.6. TUNEL staining assay

The chondrocyte death in cartilage tissue was assessed using the TUNEL apoptosis assay kit (Beyotime), according to the manufacturer's protocol. Cartilage specimens or cells were briefly fixed with 4% paraformaldehyde, then embedded in paraffin, and sectioned at 5 μm. The sections were then deparaffinized with xylene and ethanol, and the cells were rehydrated with proteinase K. After being washed three times with PBS, the sections were incubated with a TUNEL reaction mixture for 2 h at 37 °C in a moist chamber. Nuclei were stained with DAPI. Images were acquired using a Leica DM4000 B epifluorescence microscope (Leica Microsystems GmbH).

2.7. ATDC5 cell culture

The chondrogenic cell line, ATDC5, was purchased from the Chinese Academy of Sciences and maintained in DMEM supplemented with 10% FBS and 1% penicillin–streptomycin (Gibco; Thermo Fisher Scientific, Inc.) at 37 °C with 5% CO_2. Before further experimental processing, the ATDC5 cells were treated with ITS for 14 days. The commercial ITS (Sigma–Aldrich) containing 1.0 mg/ml recombinant insulin, 0.55 mg/ml transferrin, and 0.5 μg/ml sodium selenite at a 100 × concentration. Additionally, 10 ng/mL Transforming growth factor-beta 1 (TGF-β1) was added to the ITS before induction medium was added to the cell culture dish.

2.8. ATDC5 cell treatment

In order to explore the effect of inflammatory cytokines on the ferroptosis of ATDC5 cells, the cells were treated with IL-1β (10 ng/ml) and TNF-α (10 ng/ml) for 24 h. In order to study whether the activation or inhibition of ferroptosis was successful and the effect on the expression of target genes, using different concentrations of ferroptosis agonist erastin (0, 5, 10, and 20 μM) or ferroptosis inhibitor Fer-1 (0, 1, 5, and 10 μM) to treat ATDC5 cells for 24 h. In the functional study of FOXO3 in vitro, the ATDC5 chondrocytes were pre-exposed to lenti-FOXO3 or shRNA targeting FOXO3 (sh-FOXO3) followed by treatment with IL-1β (10 ng/ml)

for 24 h. To assess the involvement of ferroptosis in FOXO3-mediated OA, ATDC5 chondrocytes were pretreated with sh-FOXO3, erastin (10 μM) and Fer-1 (20 μM) for 24 h.

2.9. Isolation and culture of primary chondrocytes

One-week-old C57BL/6 mice were euthanized for primary chondrocyte extraction. With the help of a microscope, the cartilage of the knee joint of the lower limb of the mouse was carefully peeled off under aseptic conditions, then shredded, put into type II collagenase, and incubated in a 37 °C incubator for 6h. Then, the digested cartilages were resuspended and inoculated in DMEM/F12 with 10% fetal bovine serum (FBS), as well as 1% streptomycin/penicillin antibiotics. The incubator was maintained at a humidified atmosphere and 5% CO2 at 37 °C. Thereafter, the medium was replaced every 1 or 2 days. When cells grew to 70%–80% density, they were digested with 0.25% EDTA, and then, transferred onto T75 at a certain density. In the P0 to P4 passage, there was no significant change in cell morphology, hence, it can be used in cell experiments. Therefore, it can be used in cell experiments.

2.10. Lentivirus transfection

Lenti-FOXO3, Lenti-sh-FOXO3, and Lenti-NC were purchased from OBiO (Shanghai, China). Expression construct of mouse FOXO3 was subcloned into pLenti-EF1-EGFP-P2A-Puro-CMV-3xFLAG-WPRE vector. Cells were transduced at 30–50% confluency. After 12 h, more than 95% of the cells were successfully transduced. The medium was changed, and the cells were passaged after 2 days. The transduction efficiency was assessed using Western blotting.

2.11. High-density culture

To assess chondrogenic differentiation, 1.5×10^5 ATDC5 or primary chondrocytes were resuspended in 10 μL of incomplete DMEM (Gibco; Thermo Fisher Scientific, Inc.) and seeded as micromasses at the bottom of a 24-well plate. The cells were allowed to adhere for 1 h at 37 °C, after which 1 ml of DMEM containing 10 ng/ml ITS and 2% FBS was added. All media were replenished every other day, and after 14 days, the micromasses were stained with alcian blue for 24 h. Digital images were captured under a light microscope at a 7.8 × magnification (Leica DM4000B; Leica Microsystems GmbH).

2.12. CCK-8 assay

A CCK-8 assay kit (Sigma–Aldrich) was used according to the manufacturer's instructions to evaluate cell viability. ATDC5 cells were briefly treated either with IL-1β (10 ng/ml) or erastin (10 μM), for 24 h, and the culture medium was replaced with a CCK-8 working solution containing a 10% CCK-8 reagent. The cells were cultured at 37 °C for 1 h. The absorbance (450 nm) of each well was measured using a microplate reader.

2.13. Malondialdehyde (MDA) measurement

Cellular MDA concentrations were determined using the lipid peroxidation MDA assay kit (S0131S, Beyotime) as per the manufacturers' instructions. After the treatments, ATDC5 cells were harvested and lysed with a radioimmunoprecipitation assay (RIPA) lysis solution. The cell lysate was centrifuged at 12,000×*g* for 5 min, and the supernatant was collected for subsequent experiments.

2.14. Glutathione (GSH) measurement

Cellular GSH levels were assessed using the GSH ratio detection assay kit (S0053, Beyotime), following the manufacturer's instructions. The GSH assay mix was added to whole-cell lysates, and the mixture was incubated in the dark for 60 min. Fluorescence was monitored at wavelengths of 490 and 520 nm, and the GSH level was calculated from a standard curve.

2.15. Intracellular reactive oxygen species (ROS) detection

The intracellular ROS content was measured by confocal scanning microscopy using DCFH-DA. Cells were seeded in six-well plates and stimulated with IL-1β (10 ng/ml), erastin (10 μM), or Fer-1 (10 μM) for 24 h, followed by staining with 10 mM DCFH-DA at 37 °C for 30 min. Finally, the stained cells were observed under a confocal scanning microscope (Leica DM4000 B).

2.16. Lipid peroxidation detection

The degree of intracellular lipid peroxidation was determined using Liperfluo staining. ATDC5 chondrocytes were seeded in six-well plates and stimulated with IL-1β (10 ng/ml), erastin (10 μM), or Fer-1 (10 μM) for 24 h, followed by staining with Liperfluo (1 mM) for 30 min at 37 °C. Immediately after washing with PBS, the cells were observed under a fluorescence microscope (Leica DM4000 B). The fluorescence intensity in the FITC channel was monitored.

2.17. FerroOrange staining

The FerroOrange probe was used to detect intracellular Fe^{2+}. After treatments with IL-1β (10 ng/ml), erastin (10 μM), or Fer-1 (10 μM) for 24 h, the ATDC5 cells were washed with PBS and treated with a FerroOrange working solution (1 μmol L^{-1}) for 30 min. Finally, the stained cells were observed under a confocal scanning microscope (Leica DM4000 B).

2.18. Western blot analysis

Cultured cells were lysed using RIPA buffer supplemented with phosphatase and protease inhibitors (Roche Diagnostics). The protein was quantified using the BCA assay (Thermo Fisher Scientific, Inc.), and then equal quantities of extracted proteins (20–30 μg) were separated by 14–20% SDS-PAGE and electroblotted onto 0.22-μm PVDF membranes (Millipore, Sigma). Membranes were blocked with 5% BSA-PBS (Beyotime Institute of Biotechnology) for 1 h and then incubated with primary antibodies against collagen II (Abcam, ab34712; dilution 1:1000), GPX4 (Abcam, ab125066; dilution 1:1000), SLC7A11 (Abcam, ab175186; dilution 1:1000), MMP13 (Abcam, ab39012; dilution 1:1000), ADAMTS5 (Abcam, ab41037; dilution 1:1000), BAX (Cell Signaling Technology, D2E11; dilution 1:1000), BCL-2 (Cell Signaling Technology, #15071; dilution 1:1000), cleaved PARP (Cell Signaling Technology, D64E10; dilution 1:1000), cleaved caspase-3 (Cell Signaling Technology, Asp175; dilution 1:1000), NF-κB pathway antibody sampler kit (Cell Signaling Technology, 9936T; dilution 1:1000), and mitogen-activated protein kinase (MAPK) family antibody sampler kit (Cell Signaling Technology, 9926T; dilution 1:1000). Thereafter, the membranes were washed with TBS–0.1% Tween 20 (TBST) and subsequently incubated with an anti-rabbit IgG (H + L) secondary antibody (cat. no. 5151; DyLight™ 800 4X PEG conjugate; Cell Signaling Technology, 1:5000) for 1 h in the dark. After the membranes were washed with TBST, protein immunoreactivity was detected using an Odyssey fluorescence imaging system (LI-COR Biosciences). Semiquantitative analysis of the intensity of protein bands was conducted using the ImageJ V1.8.0 software (National Institutes of Health), and the results were normalized to the intensity of the internal loading control, β-actin.

2.19. IF staining in cells

ATDC5 cells were fixed with cold 4% paraformaldehyde for 20 min, treated with 0.5% Triton X-100 for 5 min, blocked with 10% goat serum

at room temperature for 60 min, and finally incubated with primary antibodies against collagen II (Abcam, ab34712; dilution 1:50) and GPX4 (Abcam, ab125066; dilution 1:100) at 4 °C for 16 h. On the following day, the slides were washed with PBS and incubated with a recombinant Alexa Fluor® 555 anti-M6PR antibody (Abcam ab203438) for 50 min in the dark. Subsequently, the slides were washed with PBS and incubated with a DAPI solution (Sigma–Aldrich, Merck KGaA) for 5 min in the dark to stain the cell nuclei. After a final wash with PBS, the samples were air-dried and sealed with anti-fluorescence quenching tablets. Digital fluorescence images were captured using a Leica DM4000 B epifluorescence microscope (Leica Microsystems GmbH) at 10 × and 20 × magnifications, and IOD measurements were obtained using the Image Pro Plus software (version 6.0; Media Cybernetics, Inc.).

2.20. Statistical analysis

All data are presented as the mean ± SD values. The GraphPad Prism software (version 9.0; GraphPad Software, San Diego, CA, USA) was used for statistical analysis. The Student's *t*-test was used for comparisons between two groups, and one- or two-way ANOVA with Sidak's multiple comparisons test was used for comparisons among more than two groups. Statistical significance was set at $P < 0.05$.

3. Results

3.1. IL-1β and TNF-α induce ferroptosis-related changes in ATDC5 chondrocytes

We first tested the levels of GSH, which is critical for the prevention of ferroptosis [25], and found that GSH levels were reduced in ATDC5 chondrocytes in response to IL-1β and TNF-α treatment (Fig. 1A). In addition, the levels of MDA, a by-product of lipid peroxidation, were reduced in the inflammatory microenvironment induced by IL-1β and TNF-α (Fig. 1B). GPX4, the key regulator of ferroptosis, is a lipid hydroperoxidase that decelerates lipid peroxidation [26]. Therefore, we examined GPX4 levels by Western blotting to detect changes in ferroptosis at the protein level in the inflammatory microenvironment. The results showed that GPX4 was significantly downregulated in ATDC5 cells after IL-1β or TNF-α treatment (Fig. 1C and D). SLC7A11 was selected as another marker of ferroptosis, and changes in its levels in the inflammatory microenvironment were consistent with those of GPX4 (Fig. 1C and D). Results from immunofluorescence also indicated that lipid peroxides could also be accumulated by IL-1β or TNF-α treatment (Fig. 1E and F). These results confirmed an increase in ferroptosis in ATDC5 chondrocytes in an in vitro inflammatory environment.

3.2. FOXO3 is associated with ferroptosis in ATDC5 chondrocytes

As FOXO3 plays a critical role in regulating oxidative stress and autophagy [27,28], we explored the effects of the ferroptosis inducer erastin and the ferroptosis inhibitor Fer-1 on FOXO3 protein expression to determine whether FOXO3 plays a pivotal regulatory role during ferroptosis. Our results showed that the levels of ferroptosis markers such as GPX4 and SLC7A11 were downregulated in ATDC5 cells treated with erastin, as the concentration of erastin increased. The trend of the changes in the FOXO3 levels was consistent with that of the ferroptosis markers, and the downregulation of FOXO3, compared with its expression level in the control group, was the most significant at 20 μM erastin (Fig. 1G and H). In the experimental group treated with Fer-1, the changes in the levels of the FOXO3 protein and the ferroptosis markers exhibited opposite trends (Fig. 1I and J). These results strongly suggest that FOXO3 plays a role in chondrocyte ferroptosis and prompted us to explore FOXO3-regulated ferroptosis in OA.

3.3. FOXO3 regulates the extracellular matrix (ECM) metabolism and apoptosis in ATDC5 chondrocytes

The degradation of the ECM and the apoptosis of chondrocytes are important features in the development of OA. Therefore, we explored the levels of ECM-related proteins (collagen II, ADAMTS5, and MMP13) and apoptosis-related proteins (BAX, cleaved caspase-3, BCL-2, and cleaved PARP) using Western blotting. Lenti-FOXO3 (lv-FOXO3) and Lenti-sh-FOXO3 (sh-FOXO3) were used for FOXO3 overexpression and knockdown in ATDC5 chondrocytes, respectively.

First, we transfected cells with the sh-FOXO3 construct and demonstrated successful FOXO3 knockdown by Western blotting (Fig. 2A and B). Next, we verified the effect of FOXO3 knockdown on the chondrogenic ability of ATDC5 chondrocytes using high-density cell culture and alcian blue staining. The results showed that FOXO3 knockdown attenuated the chondrogenic ability of ATDC5 cells (Fig. 2C, Fig. S1), while ADAMTS5 and MMP13 expressions increased and that of collagen II decreased (Fig. 2D and E). The results also showed that the knockdown of FOXO3 promoted apoptosis, which was manifested in the upregulation of BAX, cleaved caspase-3, and cleaved PARP and downregulation of BCL-2 (Fig. 2F and G). TUNEL staining also supported the promotion of apoptosis by FOXO3 knockdown (Fig. 2H, Fig. S3). IF analysis of collagen II expression further confirmed that FOXO3 mediated ECM degradation (Fig. 2I).

Subsequently, the overexpression of FOXO3 was confirmed in ATDC5 chondrocytes after lv-FOXO3 transfection (Fig. 3A and B). Alcian blue staining demonstrated that the intracellular overexpression of FOXO3 reversed the reduction of collagen accumulation caused by IL-1β (Fig. 3C, Fig. S2). The overexpression of FOXO3 also significantly reversed the effect of IL-1β stimulation on both ECM catabolism and apoptosis (Fig. 3D–G). The results of TUNEL staining and IF staining for collagen II were consistent with those of Western blotting (Fig. 3H, I, Fig. S4). In conclusion, FOXO3 overexpression inhibited ECM degradation and apoptosis in ATDC5 cells.

3.4. FOXO3 suppresses IL-1β-induced ferroptosis in ATDC5 chondrocytes

Western blotting showed that the overexpression of FOXO3 reversed the IL-1β-induced downregulation of the ferroptosis markers (Fig. 4A and B); this was further confirmed by IF staining for GPX4 (Fig. 4C and D), suggesting a regulatory effect of FOXO3 on ferroptosis in ATDC5 cells.

Next, the reversal effect of FOXO3 overexpression on ferroptosis was verified using various indicators. The results showed that the IL-1β-triggered accumulation of ROS and lipid peroxidation were inhibited by lv-FOXO3 treatment (Fig. 4E–G). The ferrous (Fe^{2+}), ferric (Fe^{3+}), and total (Fe) iron concentrations increased significantly under conditions of ferroptosis activation, one of its major features. The fluorescence intensity with FerroOrange, a Fe^{2+}-specific probe, was significantly enriched in cells treated with IL-1β, but this iron-increasing effect could also be reversed by lv-FOXO3 treatment (Fig. 4E, H). The same trends were observed for MDA and GSH (Fig. 4I and J). Furthermore, the reversal effect of lv-FOXO3 transfection on IL-1β-treated ATDC5 cells was the same as described above (Fig. 4K). These results demonstrate that ferroptosis plays a crucial role in IL-1β-induced ATDC5 chondrocyte death in vitro and confirm a reversal effect of FOXO3 on this form of cell death.

3.5. FOXO3 knockdown increases the sensitivity of ATDC5 chondrocytes to ferroptosis

We first studied the effects of the classical ferroptosis agonist erastin on the expression of matrix metalloproteinases and collagen II. Western blotting showed that the activation of ferroptosis promoted the expression of MMP13 and ADAMTS5 but inhibited that of collagen II. These

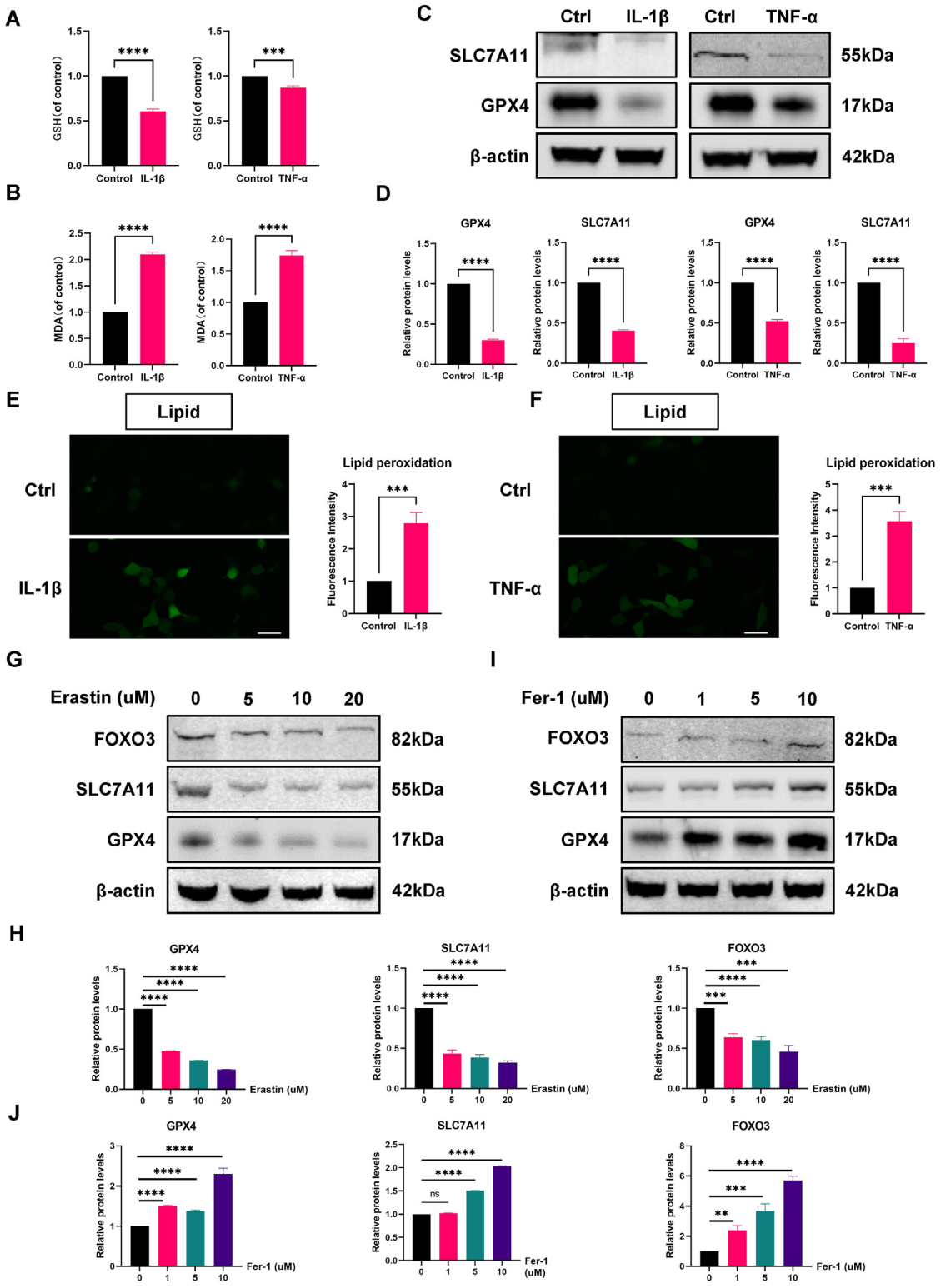

Figure 1. Inflammation can induce ferroptosis in ATDC5 cells, and FOXO3 is involved (A) Measurement of GSH content 24 h post IL-1β (10 ng/ml) or TNF-α (10 ng/ml) treatment (B) Measurement of MDA content 24h post IL-1β (10 ng/ml) or TNF-α (10 ng/ml) treatment (C) The expression level of GPX4 and SLC7A11 in ATDC5 cells were determined by WB analysis. (D) Semiquantitative analysis of GPX4 and SLC7A11 expression based on WB analysis (E) Detection of intracellular lipid peroxidation by Liperfluo fluorescence probe (scale bar: 50 μm). Semiquantitative analysis of the fluorescence intensity of lipid peroxidation (F) Detection of intracellular lipid peroxidation by Liperfluo fluorescence probe (scale bar: 50 μm). Semiquantitative analysis of the fluorescence intensity of lipid peroxidation(G) After treatment of ATDC5 cells with different concentrations of erastin (24h), FOXO3, GPX4 and SLC7A11 were determined by WB analysis (H) Semiquantitative analysis of FOXO3, GPX4 and SLC7A11 expression based on WB analysis. (I) After treatment of ATDC5 cells with different concentrations of Fer-1 (24h), FOXO3, GPX4 and SLC7A11 were determined by WB analysis. (J) Semiquantitative analysis of FOXO3, GPX4 and SLC7A11 expression based on WB analysis. *P < 0.05; **P < 0.01; ***P < 0.001; ****P < 0.0001. All data are from n = 3 independent experiments.

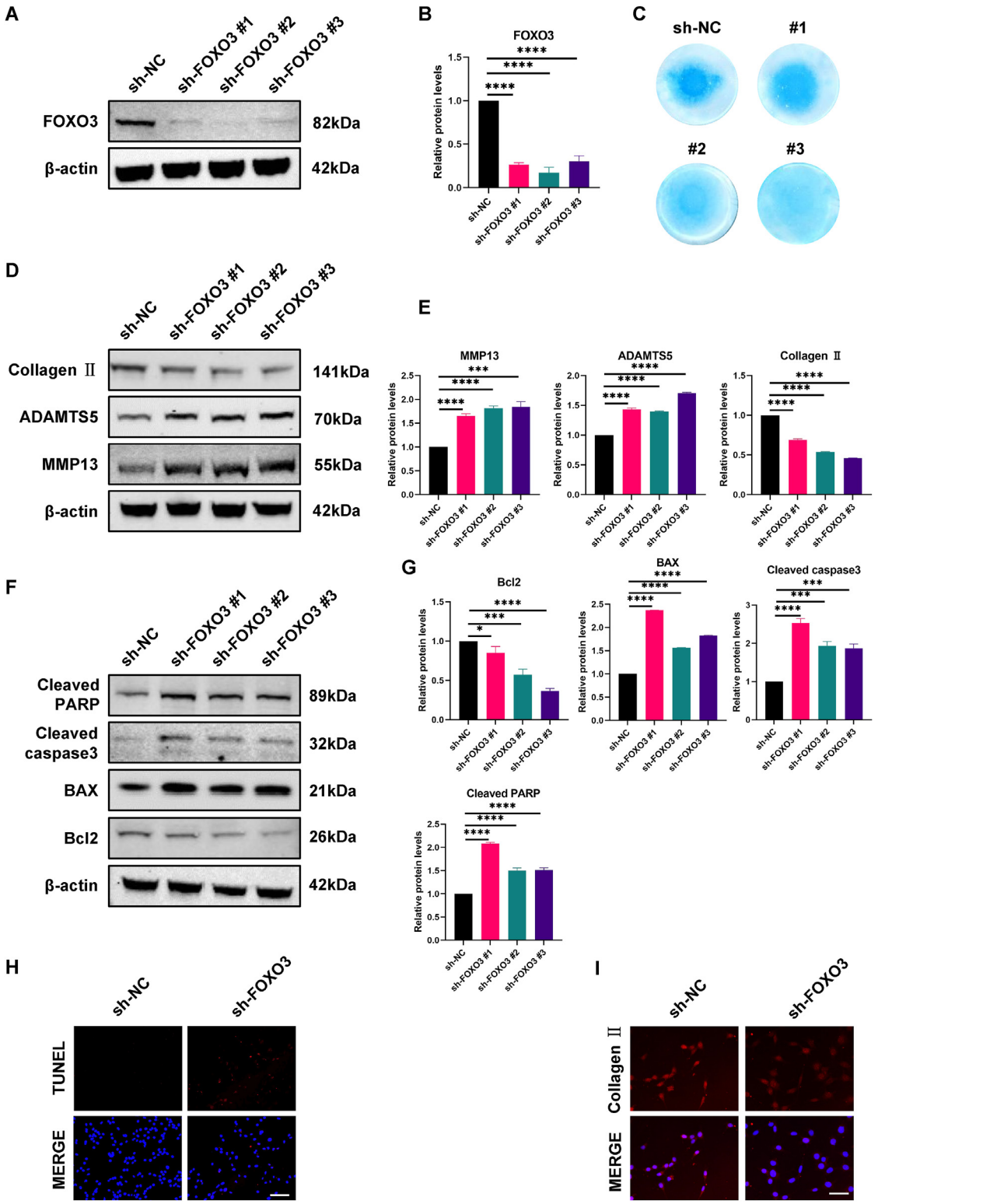

Figure 2. Knockdown of FOXO3 promotes ECM metabolic disorder and apoptosis (A) WB analysis verified the success of three lenti-sh-FOXO3 knockdown of FOXO3 in ATDC5 cells. (B) Semiquantitative analysis of FOXO3 expression based on WB analysis (C) Alcian blue staining of shRNA-treated ATDC5s. (D) Protein levels of MMP13, ADAMTS5 and Collagen II in ATDC5s infected with FOXO3 shRNA #1#2/#3 lentivirus or control shRNA lentivirus (E) Semiquantitative analysis of MMP13, ADAMTS5 and Collagen II expression based on WB analysis. (F) Protein levels of BAX, cleaved-caspase-3, BCL-2 and cleaved-PARP in ATDC5s infected with FOXO3 shRNA #1#2/#3 lentivirus or control shRNA lentivirus (G) Semiquantitative analysis of BAX, cleaved-caspase-3, BCL-2 and cleaved-PARP expression based on WB analysis. (H) TUNEL staining assay was conducted on the ATDC5 chondrocytes infected with FOXO3 shRNA #1 lentivirus or control shRNA lentivirus (scale bar: 100 μm). (I) Immunofluorescence staining of Collagen II in ATDC5 chondrocytes (scale bar: 50 μm). *P < 0.05; ***P < 0.001; ****P < 0.0001. All data are from n = 3 independent experiments. (For interpretation of the references to colour in this figure legend, the reader is referred to the Web version of this article.)

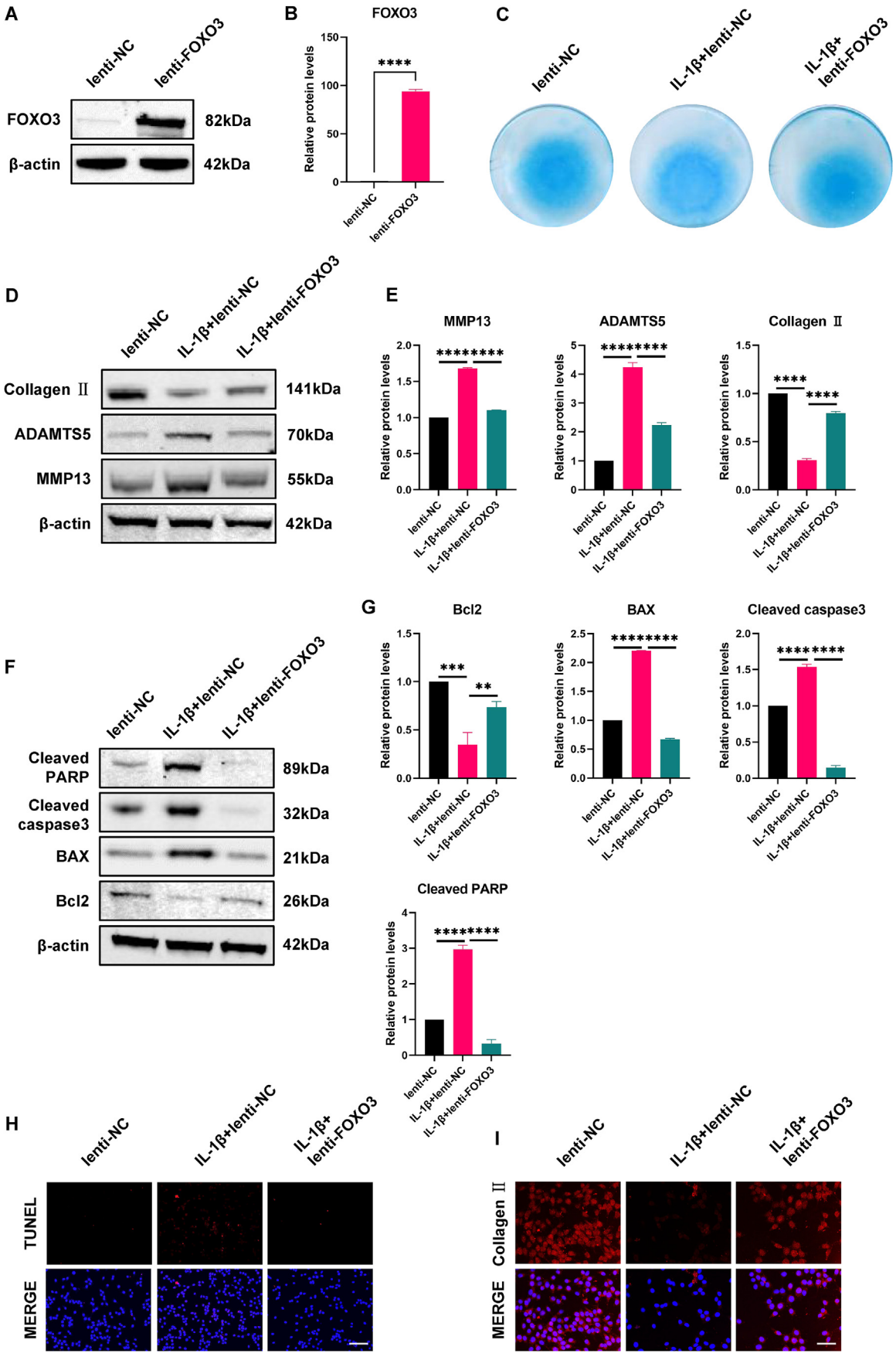

(caption on next page)

Figure 3. FOXO3 rescues IL-1β treatment-induced disturbance of extracellular matrix metabolism and apoptosis (A) WB analysis verified the success of overexpression of FOXO3 in ATDC5 cells treated with lenti-FOXO3. (B) Semiquantitative analysis of FOXO3 expression based on WB analysis (C) Alcian blue staining of lenti-FOXO3 treated ATDC5s. (D) Protein levels of MMP13, ADAMTS5 and Collagen II in ATDC5s infected with FOXO3 lentivirus and IL-1β (10 ng/ml) (E) Semiquantitative analysis of MMP13, ADAMTS5 and Collagen II expression based on WB analysis. (F) Protein levels of BAX, cleaved-caspase-3, BCL-2 and cleaved-PARP in ATDC5s infected with FOXO3 lentivirus and IL-1β (10 ng/ml) (G) Semiquantitative analysis of MMP13, ADAMTS5 and Collagen II expression based on WB analysis. (H) TUNEL staining assay was conducted on the ATDC5 chondrocytes infected with FOXO3 lentivirus and IL-1β (10 ng/ml) (scale bar: 100 μm) (I) Immunofluorescence staining of Collagen II in ATDC5 chondrocytes (scale bar: 50 μm). **P < 0.01; ***P < 0.001; ****P < 0.0001. All data are from n = 3 independent experiments. (For interpretation of the references to colour in this figure legend, the reader is referred to the Web version of this article.)

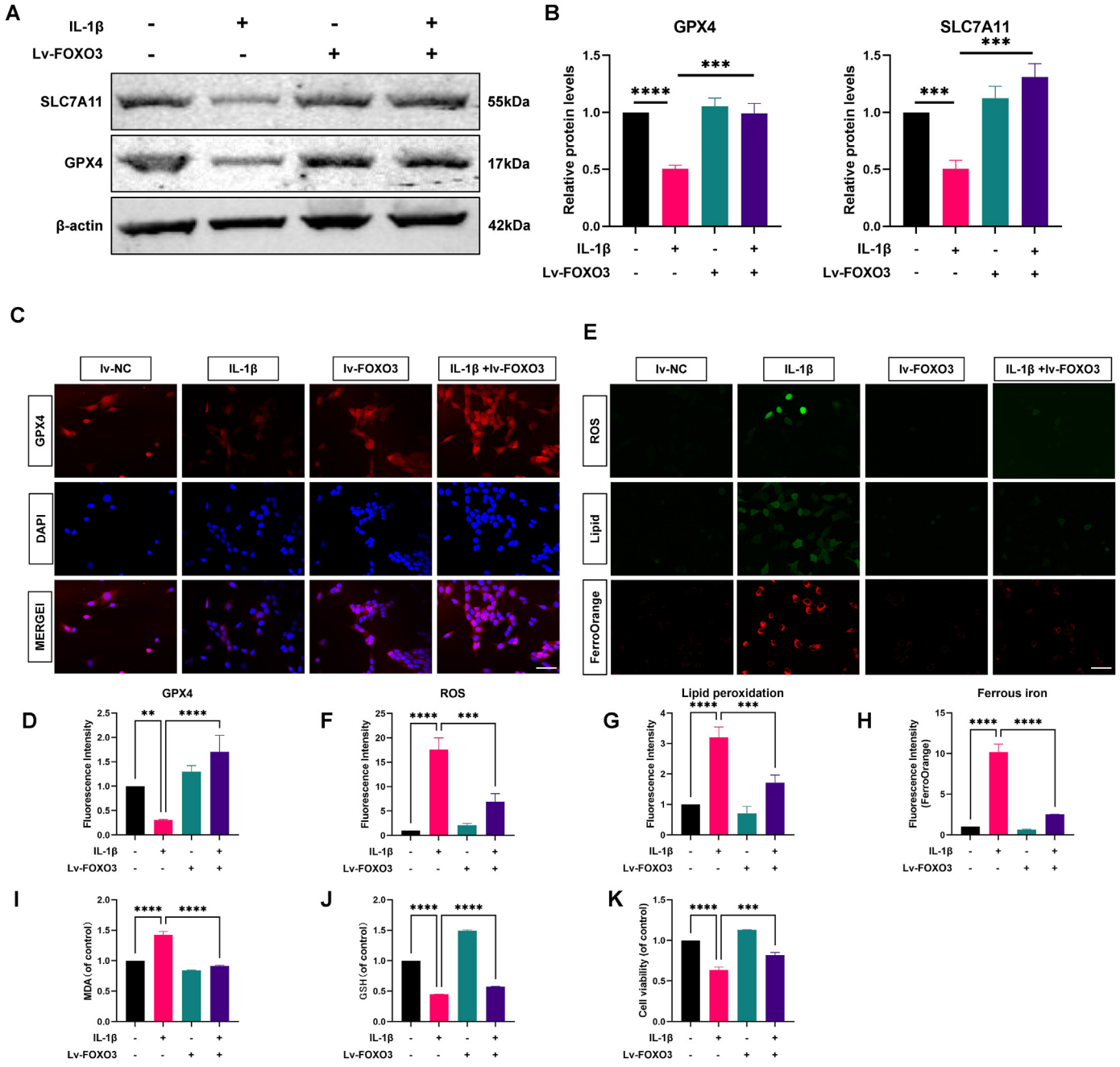

Figure 4. FOXO3 suppresses IL-1β-induced ferroptosis in ATDC5 chondrocytes (A) Protein levels of GPX4 and SLC7A11 in ATDC5s infected with FOXO3 lentivirus and IL-1β (10 ng/ml) (B) Semiquantitative analysis of GPX4 and SLC7A11 expression based on WB analysis. (C) Immunofluorescence staining of GPX4 in ATDC5 chondrocytes as treated above (scale bar: 50 μm) (D) Semiquantitative analysis of the fluorescence intensity of GPX4. (E) Detection of intracellular ROS by DCFH-DA (Up), detection of intracellular lipid peroxidation by Liperfluo fluorescence probe (Middle), detection of intracellular Fe^{2+} by FerroOrange Assay (Down) (scale bar: 50 μm). Semiquantitative analysis of the fluorescence intensity of intracellular ROS (F), lipid peroxidation (G) and intracellular Fe^{2+} (H) (I) MDA levels in ATDC5 cells were quantitatively determined using an MDA assay kit. (J) GSH levels in ATDC5 cells were quantitatively determined using an GSH assay kit (K) The cell counting kit-8 (CCK-8) assay detects cell viability. **P < 0.01; ***P < 0.001; ****P < 0.0001. All data are from n = 3 independent experiments.

effects of erastin on ATDC5 cells were more pronounced when cells were simultaneously transfected with sh-FOXO3 (Fig. 5A and B). However, the activation of ferroptosis and the in vitro OA-promoting effect of the FOXO3 knockdown were reversed by the ferroptosis inhibitor Fer-1 (Fig. 5A and B). GPX4 IF staining confirmed these results (Fig. 5C and D).

Indicators of ferroptosis, such as intracellular ROS production and lipid peroxidation, confirmed the activation of ferroptosis by erastin. In addition, the knockdown of FOXO3 enhanced the fluorescence intensity in the ROS and lipid peroxidation assays (Fig. 5E–G). The knockdown of FOXO3 also increased the accumulation of intracellular iron upon erastin treatment (Fig. 5E–H); however, these effects were all reversed by Fer-1 (Fig. 5E–H). The same trends were observed for the MDA, GSH, and cell viability indicators measured by the CCK-8 assay (Fig. 5I–K). Therefore, the results of both the inhibition and activation of FOXO3 suggest its essential role in IL-1β- or erastin-induced ATDC5 chondrocyte ferroptosis and ECM catabolism.

3.6. Erastin activates ferroptosis by targeting NF-κB and mitogen-activated protein kinase (MAPK) signaling

Although we explicitly demonstrated the essential role of FOXO3 in ferroptosis, the mechanism by which FOXO3 mediated the erastin-stimulated ferroptosis remained unclear. Ferroptosis is closely related to the activation of the NF-κB signaling pathway [19,21]. Western blotting analysis of ATDC5 chondrocytes revealed that erastin markedly activated the phosphorylation of IKK, IκBα, and p65 in the NF-κB signaling pathway (Fig. 6A and B). However, the activation of NF-κB signaling by erastin, similar to its activation of ferroptosis, could be reversed by the overexpression of FOXO3, suggesting that FOXO3 is involved in erastin-activated ferroptosis through the NF-κB signaling pathway (Fig. 6C).

Previous studies have reported that MAPKs may play an important role in the mechanism of ferroptosis [19,29]. Therefore, we hypothesized that the MAPK signaling pathway might play a role in the reversal effect of FOXO3 on erastin-induced ferroptosis in ATDC5 chondrocytes. As shown in Fig. 6A and B, the erastin treatment dose- and time-dependently promoted the phosphorylation of ERK, JNK, and p38, which indicated that the MAPK pathway played a role in the regulation of ferroptosis in ATDC5 chondrocytes. Our findings further showed that the activation of the MAPK signaling pathway by erastin was reversed in Lenti-FOXO3-transfected cells (Fig. 6F). In addition, only the overexpression of FOXO3 alone did not cause changes in the NF-κB/MAPK signaling pathway, which further suggested that the regulatory effect of FOXO3 on the NF-κB/MAPK signaling pathway needs to be realized under the premise of ferroptosis activation (Fig. 6G).

In order to further strengthen the conclusion that MAPK signaling and NF-κB signaling are involved in the regulation of ferroptosis, we further introduced inhibitors of MAPK signaling and NF-κB signaling, namely MAPK-IN-1 and NF-κB -IN-1. The results of Western blotting showed that the protein levels of GPX4 and SLC7A11 down-regulated by erastin could be significantly reversed under the premise of combined use of MAPK inhibitors (Fig. 6H and I). Co-administration of MAPK inhibitors similarly downregulated MDA, which was upregulated during ferroptosis activation, and similarly promoted the upregulation of GSH (Fig. 6L and M). The conclusion consistent with the use of MAPK inhibitors can also be obtained under the premise of using NF-κB inhibitors (Fig. 6J, K, N, O). The above results undoubtedly illustrate the direct role of NF-κB/MAPK signaling pathway in the activation of ferroptosis, and further strengthen the conclusion that FOXO3 protects cells from ferroptosis by inhibiting the activation of the NF-κB/MAPK signaling pathway.

3.7. FOXO3 also regulates ferroptosis in primary mouse chondrocytes

Although the ATDC5 cell line has superior chondrocyte properties and is widely used in the study of the musculoskeletal system. However, ferroptosis, as a novel and understudied new cell death mechanism in OA disease, we think it is very necessary to further strengthen our research conclusions through mouse primary chondrocyte culture and a series of related experiments. As expected, primary chondrocytes also showed significant down-regulation of GPX4 and SLC7A11 levels after classical inflammatory cytokine stimulation (Fig. 7A and B). In addition, after the ferroptosis agonist erastin was applied to primary chondrocytes, the levels of GPX4 and SLC7A11 were also significantly down-regulated, indicating that erastin can promote ferroptosis in primary chondrocytes (Fig. 7C and D). At the same time, while erastin promoted ferroptosis in chondrocytes, it also up-regulated the levels of matrix metalloproteinases MMP13 and ADAMTS5, and down-regulated the expression of type II collagen, suggesting that ferroptosis in primary chondrocytes promotes OA (Fig. 7C and D). On the contrary, after we applied the ferroptosis inhibitor Fer-1, it showed a completely opposite trend compared with the ferroptosis agonist (Fig. 7E and F).

Next, we also transfected primary chondrocytes with FOXO3 overexpression lentivirus, and proved the success of FOXO3 overexpression in primary cells by Western blotting (Fig. 7G and H). Meanwhile, overexpression of FOXO3 in primary chondrocytes also rescued the down-regulation of ferroptosis markers GPX4 and SLC7A11 by IL-1β, as concluded in the ATDC5 cell line (Fig. 7G and H). Abnormally expressed matrix metalloproteinases and type II collagen were also rescued by intracellular overexpression of FOXO3 (Fig. 7G and H). Results from immunofluorescence experiments also indicated that lipid peroxides and cellular Fe^{2+} accumulated by IL-1β treatment could also be down-regulated by overexpression of FOXO3 in primary chondrocytes (Fig. 7I–K). The same trends were observed for MDA and GSH (Fig. 7L and M). The above experimental results from primary chondrocytes were consistent with our research conclusions obtained in ATDC5 cell line, which undoubtedly further strengthened the conclusion of the mechanism we studied.

3.8. FOXO3 overexpression alleviates erastin-exacerbated OA in mice

Considering that FOXO3 had inhibitory effects on IL-1β-mediated ferroptosis activation and erastin-promoted induction of matrix-degrading enzymes in vitro, we investigated a possible effect of FOXO3 on catabolic genes and the expression of key ferroptosis genes in vivo and in subsequent OA pathogenesis. Erastin, Lenti-FOXO3, and an equivalent volume of the vehicle were injected into the knee joint of mice with surgery-induced OA (Fig. 8A). The mice were sacrificed and their knee joints were harvested 8 weeks after DMM surgery. First, we performed micro-CT analysis of the undecalcified bone samples. As shown in Fig. 8B, the mice in the DMM group exhibited signs of joint deformity, including joint space narrowing and osteophyte formation. These characteristics were more pronounced in the erastin injection group, whereas osteophyte formation and joint space narrowing were significantly alleviated after Lenti-FOXO3 injection. Furthermore, the results of micro-CT also showed that compared with the injection of erastin, the injection of erastin plus Lenti-FOXO3 raised the BV/TV, Tb. N, and Tb. Th of subchondral bone, and lessened Tb. Sp (Fig. 8C). Assessment of the cartilage destruction using H&E and safranin-O staining (Fig. 8D) revealed wear in the articular surface and degeneration and disappearance of the cartilage layer in the DMM surgery group, which was more conspicuous in the erastin injection group. However, the injection of the FOXO3-encoding lentivirus showed a certain rescue effect against the damage of the articular surface (Fig. 8D). In the DMM mice injected with Lenti-FOXO3, the OARSI score was significantly improved compared with those in the DMM and erastin-treated groups (Fig. 8E). TUNEL staining suggested that erastin promoted articular surface damage by aggravating chondrocyte death, while FOXO3 overexpression contributed to rescuing cells from death (Fig. 8F and G). Further, we examined the possible effects of intra-articular injection of Lenti-FOXO3 on GPXP4 expression and collagen II levels in cartilage tissues after DMM surgery. FOXO3 was almost undetectable in the DMM-induced OA knee but was highly detected in mice injected with the lentivirus encoding mouse FOXO3 (Fig. 8H and I).

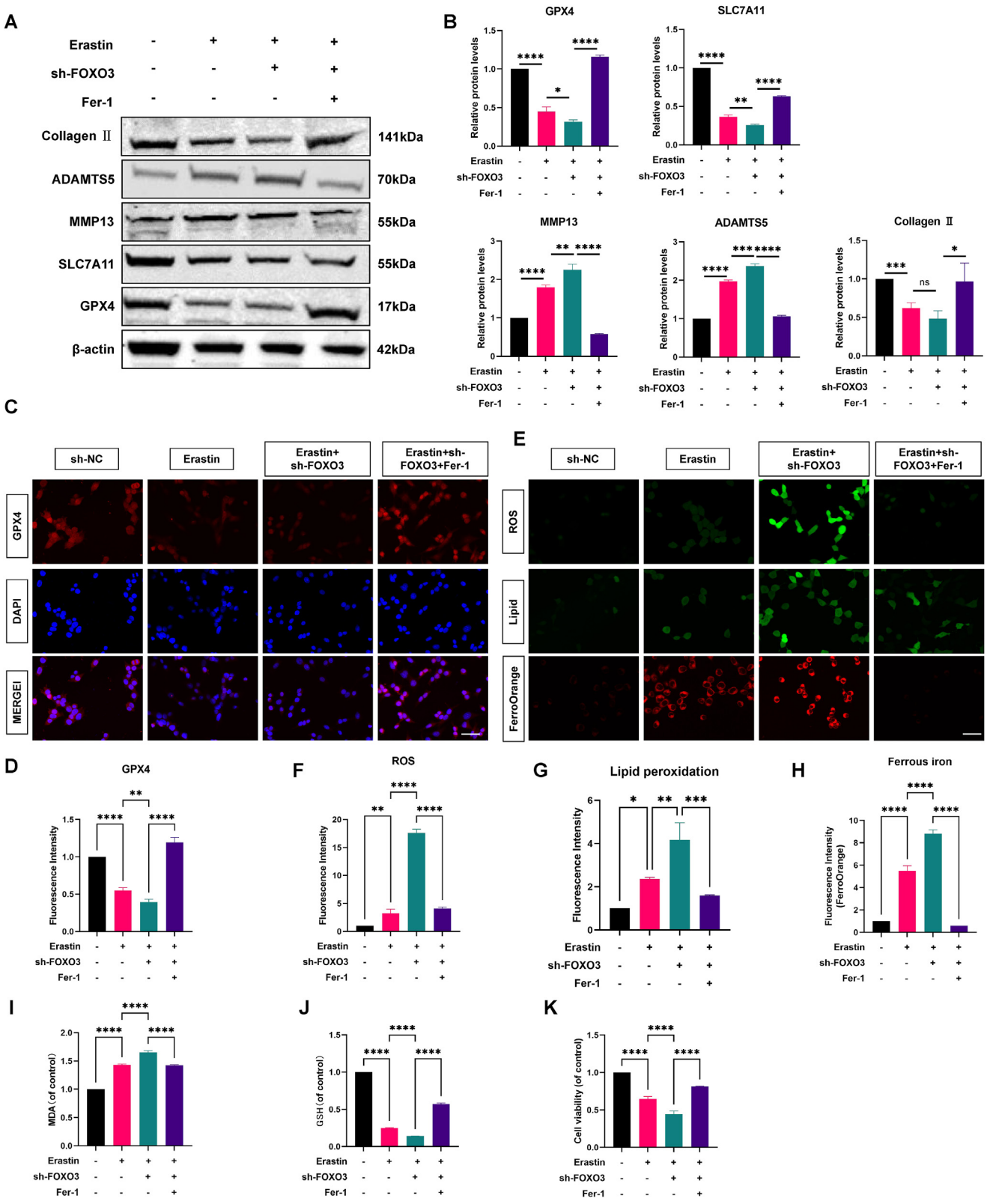

Figure 5. FOXO3 knockdown increased the sensitivity of ATDC5 chondrocytes to ferroptosis (A) Protein levels of GPX4, SLC7A11, MMP13, ADAMTS5 and Collagen II in ATDC5s infected with erastin (10 μM), Fer-1 (10 μM) and sh-FOXO3 (B) Semiquantitative analysis of protein expression based on WB analysis. (C) Immunofluorescence staining of GPX4 in ATDC5 chondrocytes as treated above (scale bar: 50 μm) (D) Semiquantitative analysis of the fluorescence intensity of GPX4. (E) Detection of intracellular ROS by DCFH-DA (Up), detection of intracellular lipid peroxidation by Liperfluo fluorescence probe (Middle), detection of intracellular Fe^{2+} by FerroOrange Assay (Down) (scale bar: 50 μm). Semiquantitative analysis of the fluorescence intensity of intracellular ROS (F), lipid peroxidation (G) and intracellular Fe^{2+} (H) (I) MDA levels in ATDC5 cells were quantitatively determined using an MDA assay kit. (J) GSH levels in ATDC5 cells were quantitatively determined using an GSH assay kit (K) The cell counting kit-8 (CCK-8) assay detects cell viability. *P < 0.05; **P < 0.01; ***P < 0.001; ****P < 0.0001. All data are from n = 3 independent experiments.

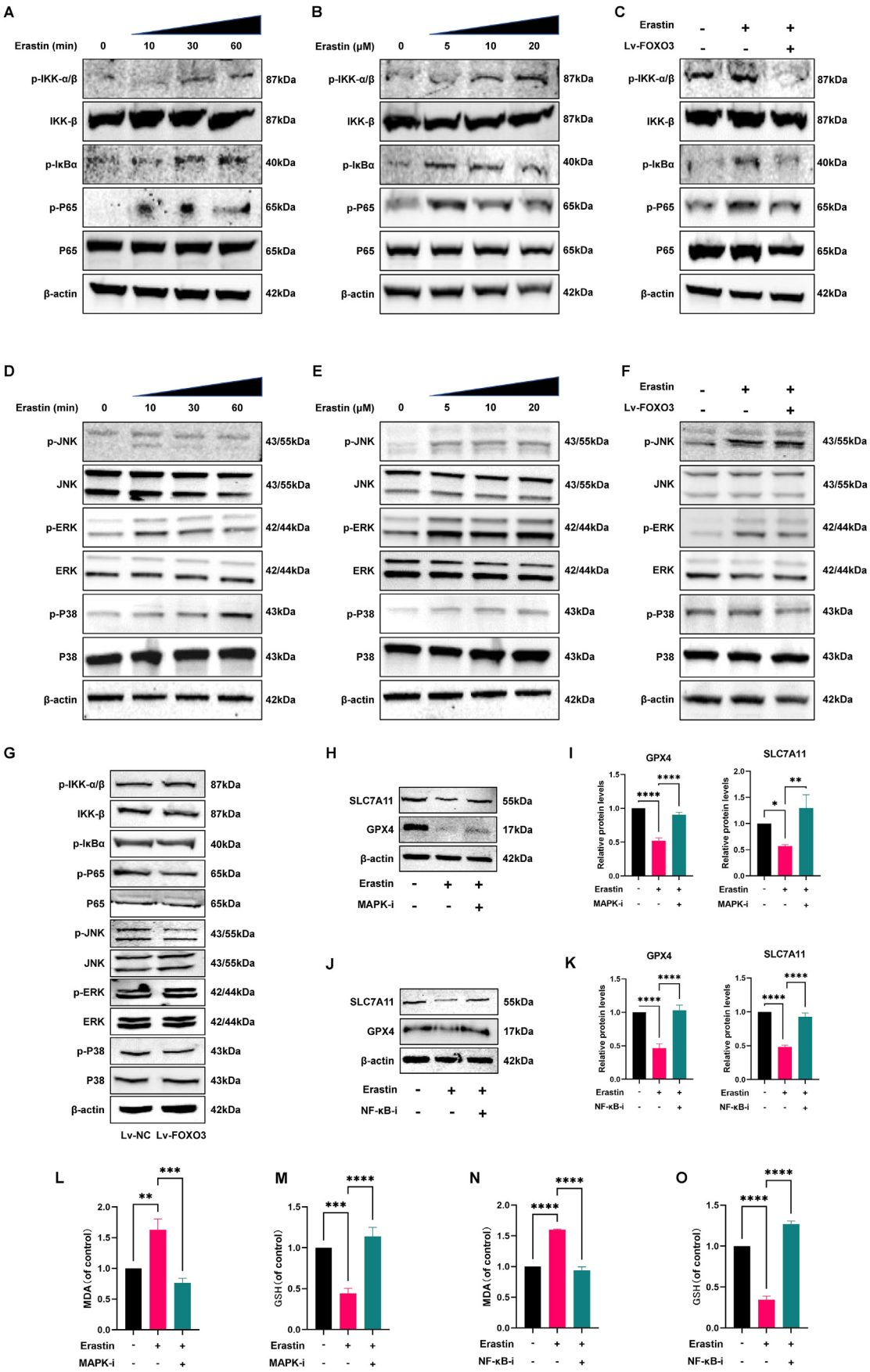

(caption on next page)

Figure 6. Erastin activates ferroptosis by targeting NF-κB and MAPK signaling (A) Western blotting showed that erastin affected NF-κB signal-related proteins IKK/p-IKK, p-IκBα, and P65/p-P65 (A, B) and MAPK signal-related proteins p-JNK/JNK, p-ERK/ERK and p-P38/P38 (D, E). Overexpression of FOXO3 inhibited erastin-activated NF-κB (C) and MAPK (D) signaling (G) Effect of intracellular overexpression of FOXO3 on NF-κB/MAPK signaling pathway. (H) Protein levels of GPX4 and SLC7A11 in ATDC5s treated with erastin (10 μM) and MAPK-IN-1 (10 μM) (I) Semiquantitative analysis of GPX4 and SLC7A11 expression based on WB analysis. (J) Protein levels of GPX4 and SLC7A11 in ATDC5s treated with erastin (10 μM) and NF-κB-IN-1 (50 μM) (K) Semiquantitative analysis of GPX4 and SLC7A11 expression based on WB analysis. (L, N) MDA levels in ATDC5 cells were quantitatively determined using an MDA assay kit. (M, O) GSH levels in ATDC5 cells were quantitatively determined using an GSH assay kit. *P < 0.05; **P < 0.01; ***P < 0.001; ****P < 0.0001. All data are from n = 3 independent experiments.

Injection with Lenti-FOXO3 reversed the erastin-mediated down-regulation of GPX4 and collagen II levels (Fig. 8H, J-K). In addition, we found a similar trend in joint synovial tissue, that is, the down-regulation of GPX4 level in joint synovial tissue caused by DMM surgery could also be rescued by intra-articular injection of FOXO3-overexpressing lentivirus (Fig. S5). These results suggest that FOXO3 may be involved in OA progression through regulation of ferroptosis. Therefore, intra-articular FOXO3 delivery may be a potential approach to OA treatment.

4. Discussion

OA is a complex pathological condition associated with multiple factors, and its underlying pathogenesis has not yet been fully elucidated. Therefore, except for joint replacement, there is no effective treatment method or a molecular drug for advanced OA [1,30,31]. An increase in cell death is considered to be a hallmark of chondrocytes undergoing osteoarthritic changes. Cell death can be divided into apoptotic and

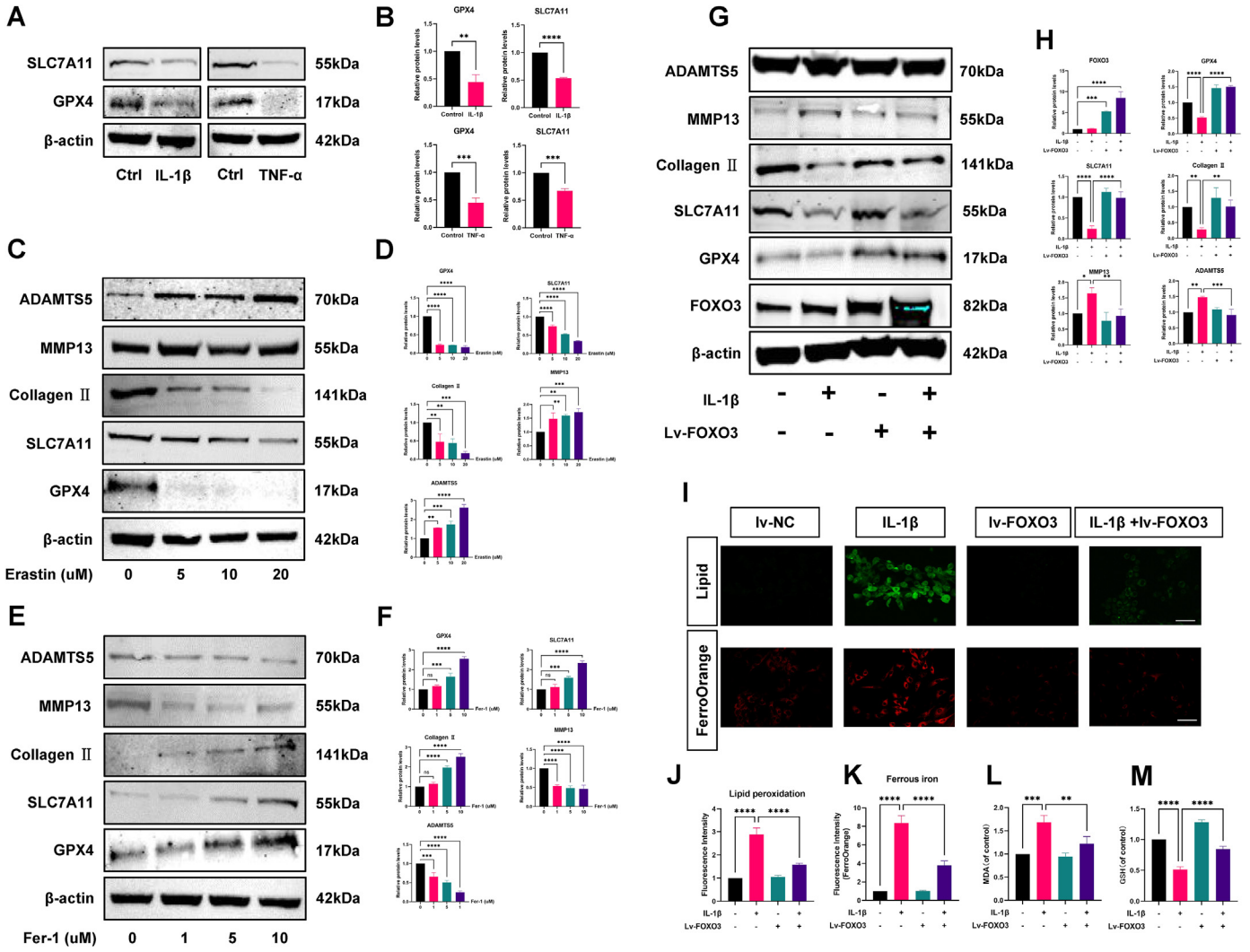

Figure 7. FOXO3 also regulates ferroptosis in primary mouse chondrocytes (A) The expression level of GPX4 and SLC7A11 in primary chondrocytes were determined by WB analysis. (B) Semiquantitative analysis of GPX4 and SLC7A11 expression based on WB analysis (C) After treatment of primary chondrocytes with different concentrations of erastin (24h), GPX4, SLC7A11, Collagen II, MMP13 and ADAMTS5 were determined by WB analysis (D) Semiquantitative analysis of F GPX4, SLC7A11, Collagen II, MMP13 and ADAMTS5 expression based on WB analysis. (E) After treatment of primary chondrocytes with different concentrations of Fer-1 (24h), GPX4, SLC7A11, Collagen II, MMP13 and ADAMTS5 were determined by WB analysis (F) Semiquantitative analysis of GPX4, SLC7A11, Collagen II, MMP13 and ADAMTS5 expression based on WB analysis. (G) Protein levels of FOXO3, GPX4, SLC7A11, Collagen II, MMP13 and ADAMTS5 in primary chondrocytes infected with FOXO3 lentivirus and IL-1β (10 ng/ml) (H) Semiquantitative analysis of FOXO3, GPX4, SLC7A11, Collagen II, MMP13 and ADAMTS5 expression based on WB analysis. (I) Detection of intracellular lipid peroxidation by Liperfluo fluorescence probe (Up), detection of intracellular Fe^{2+} by FerroOrange Assay (Down) (scale bar: 50 μm). Semiquantitative analysis of the fluorescence intensity of lipid peroxidation (J) and intracellular Fe^{2+} (K) (L) MDA levels in primary chondrocytes were quantitatively determined using an MDA assay kit. (M) GSH levels in primary chondrocytes were quantitatively determined using an GSH assay kit. *P < 0.05; **P < 0.01; ***P < 0.001; ****P < 0.0001. All data are from n = 3 independent experiments.

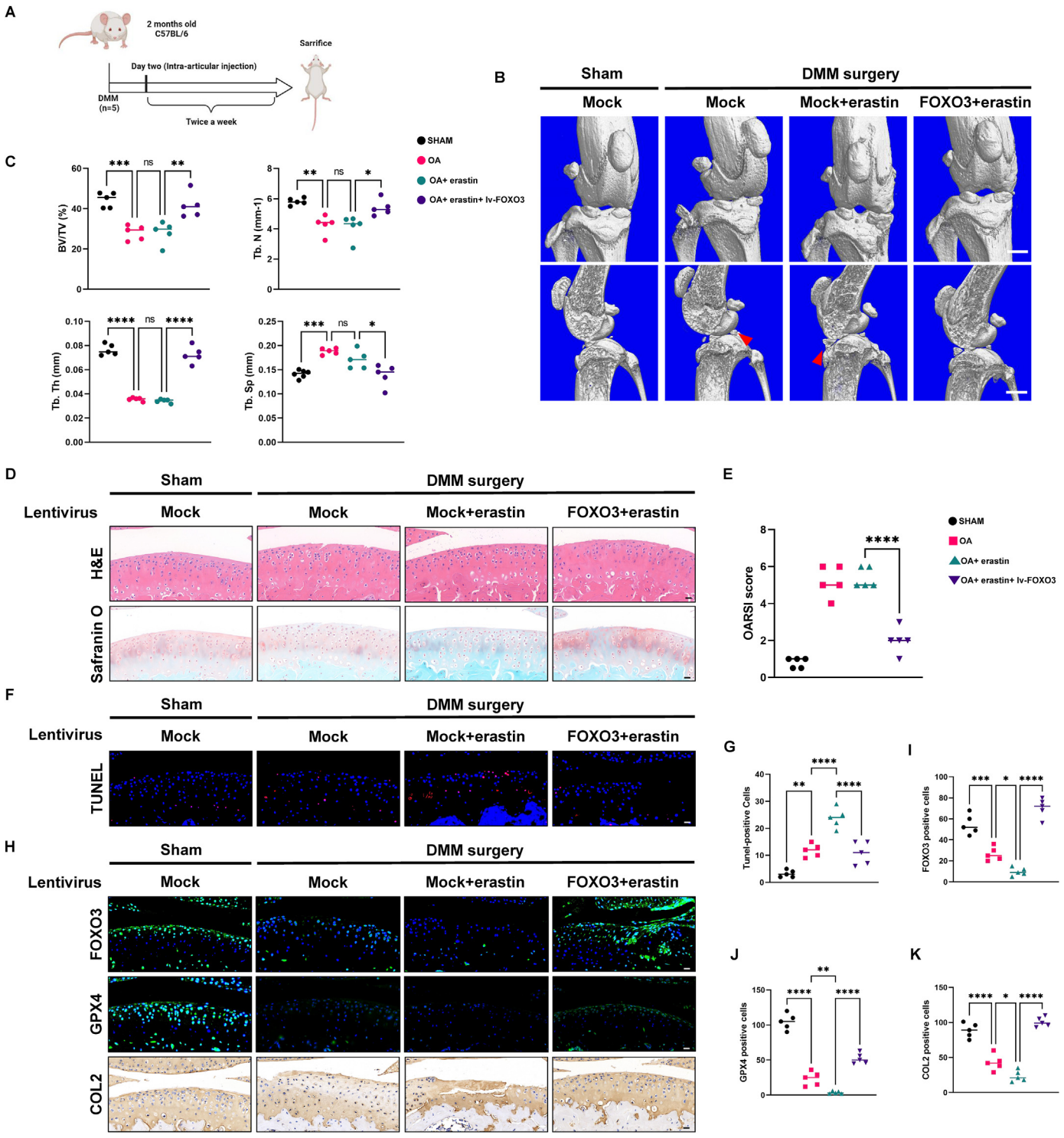

Figure 8. FOXO3 overexpression alleviates erastin-exacerbated OA in mice (A) Schematic of the time course used for the DMM-induced in vivo osteoarthritis experiments. (B) Reconstruction images of micro-CT scanning of the knees and osteophytes (red arrow). Scale bars, 1 mm (C) The BV/TV, trabecular number (Tb. N), trabecular thickness (Tb. Th), and trabecular spacing (Tb. Sp) of the subchondral bone (D) H&E staining and Safranin O and fast green staining were performed to observe the cell morphology and tissue integrity in the articular cartilage tissues of the mouse knee undergoing DMM surgery. Scale bars, 20 μm. (E) OARSI grade used for evaluation of the cartilage degradation in the four groups (F, G) TUNEL staining assay in the articular cartilage tissues of the mouse knee undergoing DMM surgery. Scale bars, 20 μm. (H– K) Representative images for FOXO3 (up), GPX4 (middle), and collagen II (down) immunostaining in cartilage tissues obtained from sham or DMM mouse knees. Scale bars, 25 μm. The bar graphs show quantification of the FOXO3-, GPX4-, or COL2-positive cells from total cell population per field, in immunohistochemical and immunofluorescence sections. *P < 0.05; **P < 0.01; ***P < 0.001; ****P < 0.0001. All data are from n = 3 independent experiments. N = 5. (For interpretation of the references to colour in this figure legend, the reader is referred to the Web version of this article.)

nonapoptotic processes, including classical modes of cell death, such as necroptosis, pyroptosis, and ferroptosis [8,9]. Numerous studies have shown that ferroptosis is associated with cell death in various diseases, including kidney, immune, metabolic, bone, and neoplastic diseases [10,11,29,32]. Several recent studies have shown that the occurrence of ferroptosis in chondrocytes and the levels of intracellular ferroptosis-inducing molecules are highly correlated with the occurrence and progression of OA [13,19,33]. In-depth examination of the mechanism of ferroptosis and of the molecular mechanism regulating ferroptosis in chondrocytes is expected to provide new targets and a therapeutic basis for the treatment of OA.

Our research data showed that the articular cartilage from the DMM surgery group of mice exhibited an increase in cell ferroptosis and the downregulation of GPX4 levels. Although chronic inflammatory diseases exhibit a high degree of complexity, an association between decreased GPX4 levels and a poor prognosis suggests that ferroptosis may be a facilitating factor contributing to the pathogenesis and progression of OA. Oxidative stress, including elevated ROS levels and increased accumulation of lipid peroxides, is the driver of chronic inflammation in joints and important indicator of OA severity [34,35]. Therefore, the regulation of cellular ferroptosis could play a role in inhibiting the progression of OA.

Through a series of in vitro experiments, we found that Fer-1, a specific inhibitor of ferroptosis, could reverse the inflammation-induced increase in ferroptosis levels and the accumulation of intracellular ROS, lipid peroxides, and iron. Furthermore, Fer-1 ameliorated the inflammation-induced disturbances in the ECM catabolism in the ATDC5 cell line. These results strongly suggest that the protection against cellular ferroptosis may play a role in alleviating OA progression. Erastin, the optimal ferroptosis inducer, aggravated the destruction of the articular cartilage in a DMM surgery-induced mouse model of OA, which was accompanied by decreased levels of ferroptosis markers such as GPX4. Thus, our data show that ferroptosis promotes OA progression.

Recent studies have shown that FOXO3 can maintain cartilage homeostasis during OA through an autophagy regulatory mechanism [36,37]. The study by Matsuzaki et al. [38] in 2019 directly revealed the important role of FOXO family in cartilage development, cartilage homeostasis maintenance and autophagy regulation in chondrocytes. In the context of intracellular knockdown of the FOXO family, it will directly lead to chondrodysplasia, accelerated wear and tear, and disorder of autophagy. As ferroptosis is an autophagy-dependent form of cell death [11,39,40], we speculated that FOXO3 might also regulate ferroptosis in chondrocytes. Indeed, ferroptosis was inhibited by FOXO3 overexpression, independently of its anti-inflammatory and antiapoptotic functions. ROS generation is an important factor in the increase of intracellular iron levels and initiation of ferroptosis [39]. Our data also showed that ROS were induced when ATDC5 chondrocytes were treated with IL-1β or erastin at different concentrations and times. In addition, the overexpression of FOXO3 antagonized ROS production under ferroptosis-promoting conditions. As a key regulator of ferroptosis, GPX4 may be a cue for cellular ferroptosis. Miao et al. [19] showed that changes in GPX4 levels were closely related to OA progression. Therefore, we investigated the effect of changes in FOXO3 levels on inflammation- and erastin-induced GPX4 expression. The results showed that both IL-1β and erastin treatment resulted in the downregulation of GPX4 at the cellular and tissue levels in both in vitro and in vivo experiments, while treatment with a FOXO3-overexpressing lentivirus ameliorated articular cartilage damage, upregulated GPX4 expression, and increased the level of the GSH substrate. The knockdown of FOXO3 aggravated the accumulation of erastin-induced ferroptosis characteristic products, such as intracellular ROS, lipid peroxides, and iron, and these effects were reversed by Fer-1. Consistently, erastin and FOXO3 knockdown disrupted ECM catabolism, which was also rescued by Fer-1. These results strongly suggest that FOXO3 alleviates OA by inhibiting cellular ferroptosis to a certain extent.

A recent study has demonstrated that TNF antagonists sensitized synovial fibroblasts to ferroptotic cell death in a mouse model of collagen-induced arthritis and uncovered a possible role of NF-κB signaling in the mechanism of ferroptosis [21]. The role of the NF-κB pathway in OA has been identified in numerous studies [41–43]. Our results also showed that NF-κB signaling was significantly activated after stimulation with erastin, whereas FOXO3 overexpression inhibited the phosphorylation of IκBα and consequently, p65. MAPKs are a serine/threonine protein kinase family containing JNK, ERK, and p38, among others, and regulating numerous cellular activities, including cell proliferation, differentiation, apoptosis, inflammation, and innate immunity [44,45]. MAPK signaling can be activated by various stressors, including oxidative stress and IL-1β. Furthermore, our results showed that erastin activated MAPK signaling, as evidenced by the phosphorylation of JNK, ERK, and p38, whereas the overexpression of FOXO3 inhibited MAPK activation. These results

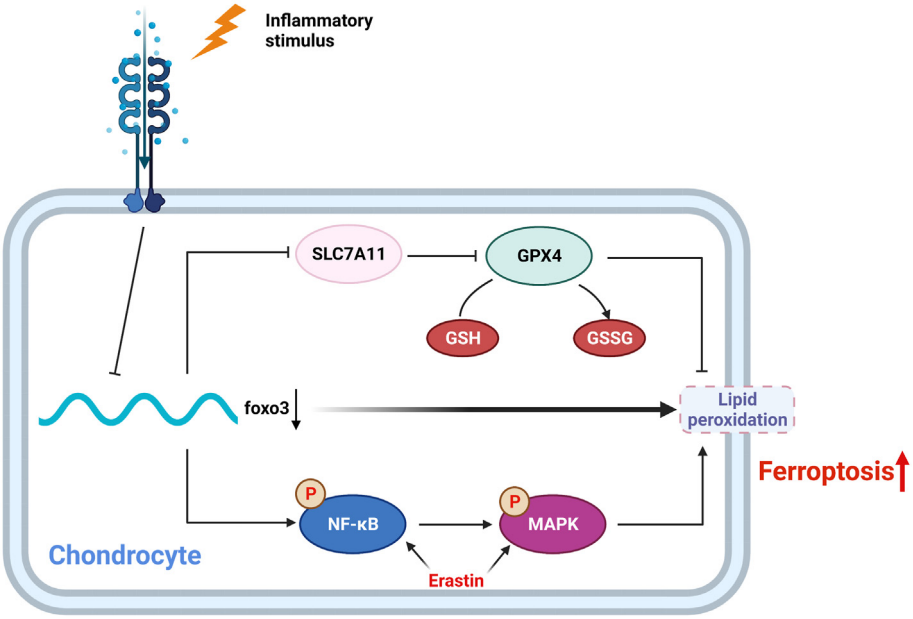

Figure 9. Schematic illustration of effect of FOXO3-regulated ferroptosis in osteoarthritis development.

indicate that FOXO3 can directly interact with the ECM catabolism disorder induced by the ferroptosis mechanism through the NF-κB/MAPK pathway, thereby exerting an anti-inflammatory effect in OA.

This study had certain limitations. Owing to the difficulty of obtaining human clinical specimens, it was not used in this study. The use of human tissue and primary cells may further validate our conclusions. In future studies, we will focus on the predictive and therapeutic role of ferroptosis in human arthritis. Furthermore, we demonstrated that FOXO3 was essential for chondrocyte ferroptosis in an inflammatory microenvironment; however, the interaction of FOXO3 with other canonical biomarkers of ferroptosis, including GPX4, remains unclear. Future research is required to unveil the inherent connections among *GPX4*, *SCL7A11*, and other genes that may be involved in ferroptosis in chondrocytes.

In conclusion, targeting ferroptosis-associated metabolism in OA may provide new targets and novel mechanisms for OA treatment. Moreover, targeting FOXO3 could efficiently reverse chondrocyte ferroptosis in OA by disrupting the vicious cycle of lipid peroxidation and iron accumulation, eventually ameliorating the destruction and degeneration of the articular cartilage. This study provides references and serves as a guide for future research on the molecular mechanisms underlying the relationship between ferroptosis and OA (Fig. 9).

Author contributions

CZ (Chen Zhao) and GS (Guantong Sun) designed the experimental plan. KK (Keyu Kong) and YL (Yaxin Li) helped refine the experimental plan. CZ completed most of the experiments and the writing of the article. XL (Xiaodong Li) and TK (Tianyou Kan) have helped with animal surgery operations. FY (Fei Yang) helped revise the draft of the article. XW (Xiaoqing Wang) and LW (Lei Wang) provided the research platform and research funding, and reviewed the research proposal. The final manuscript was approved by all authors.

Declaration of competing interest

The authors have declared that no competing interest exists.

Acknowledgments

This work was supported by the National Natural Science Foundation of China (81871791); Youth Fund Project of the National Natural Science Foundation of China (81902194).

Appendix A. Supplementary data

Supplementary data to this article can be found online at https://doi.org/10.1016/j.jot.2023.02.005.

References

[1] Barnett R. Osteoarthritis. Lancet 2018;391:10134.
[2] Bortoluzzi A, Furini F, Scire CA. Osteoarthritis and its management - epidemiology, nutritional aspects and environmental factors. Autoimmun Rev 2018;17(11):1097–104.
[3] Wan Y, Lv Y, Li L, Yin Z. 15-Lipoxygenase-1 in osteoblasts promotes TGF-beta1 expression via inhibiting autophagy in human osteoarthritis. Biomed Pharmacother 2020;121:109548.
[4] Latourte A, Kloppenburg M, Richette P. Emerging pharmaceutical therapies for osteoarthritis. Nat Rev Rheumatol 2020;16(12):673–88.
[5] Martel-Pelletier J, Wildi LM, Pelletier JP. Future therapeutics for osteoarthritis. Bone 2012;51(2):297–311.
[6] McCarberg B, Tenzer P. Complexities in the pharmacologic management of osteoarthritis pain. Curr Med Res Opin 2013;29(5):539–48.
[7] Song J, Baek IJ, Chun CH, Jin EJ. Dysregulation of the NUDT7-PGAM1 axis is responsible for chondrocyte death during osteoarthritis pathogenesis. Nat Commun 2018;9(1):3427.
[8] Stockwell BR, Friedmann Angeli JP, Bayir H, Bush AI, Conrad M, Dixon SJ, et al. Ferroptosis: a regulated cell death nexus linking metabolism. Redox Biology, and Disease, Cell 2017;171(2):273–85.
[9] Dixon SJ, Lemberg KM, Lamprecht MR, Skouta R, Zaitsev EM, Gleason CE, et al. Ferroptosis: an iron-dependent form of nonapoptotic cell death. Cell 2012;149(5):1060–72.
[10] Chen C, Wang D, Yu Y, Zhao T, Min N, Wu Y, et al. Legumain promotes tubular ferroptosis by facilitating chaperone-mediated autophagy of GPX4 in AKI. Cell Death Dis 2021;12(1):65.
[11] Dai E, Han L, Liu J, Xie Y, Kroemer G, Klionsky DJ, et al. Autophagy-dependent ferroptosis drives tumor-associated macrophage polarization via release and uptake of oncogenic KRAS protein. Autophagy 2020;16(11):2069–83.
[12] Yuan S, Wei C, Liu G, Zhang L, Li J, Li L, et al. Sorafenib attenuates liver fibrosis by triggering hepatic stellate cell ferroptosis via HIF-1alpha/SLC7A11 pathway. Cell Prolif 2022;55(1):e13158.
[13] Yao X, Sun K, Yu S, Luo J, Guo J, Lin J, et al. Chondrocyte ferroptosis contribute to the progression of osteoarthritis. J Orthop Translat 2021;27:33–43.
[14] van Vulpen LFD, Roosendaal G, van Asbeck BS, Mastbergen SC, Lafeber FPJG, Schutgens REG. The detrimental effects of iron on the joint: a comparison between haemochromatosis and haemophilia. J Clin Pathol 2015;68(8):592.
[15] Nieuwenhuizen L, Schutgens REG, van Asbeck BS, Wenting MJ, van Veghel K, Roosendaal G, et al. Identification and expression of iron regulators in human synovium: evidence for upregulation in haemophilic arthropathy compared to rheumatoid arthritis, osteoarthritis, and healthy controls. Haemophilia 2013;19(4):e218–27.
[16] Abusarah J, Bentz M, Benabdoune H, Rondon PE, Shi Q, Fernandes JC, et al. An overview of the role of lipid peroxidation-derived 4-hydroxynonenal in osteoarthritis. Inflamm Res 2017;66(8):637–51.
[17] van Gastel N, Stegen S, Eelen G, Schoors S, Carlier A, Daniels VW, et al. Lipid availability determines fate of skeletal progenitor cells via SOX9. Nature 2020;579(7797):111–7.
[18] Feng K, Ge Y, Chen Z, Li X, Liu Z, Li X, et al. Curcumin inhibits the PERK-eIF2alpha-CHOP pathway through promoting SIRT1 expression in oxidative stress-induced rat chondrocytes and ameliorates osteoarthritis progression in a rat model. Oxid Med Cell Longev 2019;2019:8574386.
[19] Miao Y, Chen Y, Xue F, Liu K, Zhu B, Gao J, et al. Contribution of ferroptosis and GPX4's dual functions to osteoarthritis progression. EBioMedicine 2022;76:103847.
[20] Zhang X, Huang Z, Xie Z, Chen Y, Zheng Z, Wei X, et al. Homocysteine induces oxidative stress and ferroptosis of nucleus pulposus via enhancing methylation of GPX4. Free Radic Biol Med 2020;160:552–65.
[21] Wu J, Feng Z, Chen L, Li Y, Bian H, Geng J, et al. TNF antagonist sensitizes synovial fibroblasts to ferroptotic cell death in collagen-induced arthritis mouse models. Nat Commun 2022;13(1):676.
[22] Glasson SS, Blanchet TJ, Morris EA. The surgical destabilization of the medial meniscus (DMM) model of osteoarthritis in the 129/SvEv mouse. Osteoarthritis Cartilage 2007;15(9):1061–9.
[23] Chen D, Shen J, Zhao W, Wang T, Han L, Hamilton JL, et al. Osteoarthritis: toward a comprehensive understanding of pathological mechanism. Bone Research 2017;5(1):16044.
[24] Laverty S, Girard CA, Williams JM, Hunziker EB, Pritzker KPH. The OARSI histopathology initiative – recommendations for histological assessments of osteoarthritis in the rabbit. Osteoarthritis Cartilage 2010;18:S53–65.
[25] Miess H, Dankworth B, Gouw AM, Rosenfeldt M, Schmitz W, Jiang M, et al. The glutathione redox system is essential to prevent ferroptosis caused by impaired lipid metabolism in clear cell renal cell carcinoma. Oncogene 2018;37(40):5435–50.
[26] Zhou Y, Zhou H, Hua L, Hou C, Jia Q, Chen J, et al. Verification of ferroptosis and pyroptosis and identification of PTGS2 as the hub gene in human coronary artery atherosclerosis. Free Radic Biol Med 2021;171:55–68.
[27] Zou DB, Mou Z, Wu W, Liu H. TRIM33 protects osteoblasts from oxidative stress-induced apoptosis in osteoporosis by inhibiting FOXO3a ubiquitylation and degradation. Aging Cell 2021;20(7):e13367.
[28] Yang H, Wen Y, Zhang M, Liu Q, Zhang H, Zhang J, et al. MTORC1 coordinates the autophagy and apoptosis signaling in articular chondrocytes in osteoarthritic temporomandibular joint. Autophagy 2020;16(2):271–88.
[29] Yang Y, Lin Y, Wang M, Yuan K, Wang Q, Mu P, et al. Targeting ferroptosis suppresses osteocyte glucolipotoxicity and alleviates diabetic osteoporosis. Bone Res 2022;10(1):26.
[30] Martel-Pelletier J, Barr AJ, Cicuttini FM, Conaghan PG, Cooper C, Goldring MB, et al. Osteoarthritis. Nat Rev Dis Prim 2016;2:16072.
[31] Glyn-Jones S, Palmer AJR, Agricola R, Price AJ, Vincent TL, Weinans H, et al. Osteoarthritis. Lancet 2015;386(9991):376–87.
[32] Ma X, Xiao L, Liu L, Ye L, Su P, Bi E, et al. CD36-mediated ferroptosis dampens intratumoral CD8(+) T cell effector function and impairs their antitumor ability. Cell Metabol 2021;33(5):1001–1012 e5.
[33] Zhou X, Zheng Y, Sun W, Zhang Z, Liu J, Yang W, et al. D-mannose alleviates osteoarthritis progression by inhibiting chondrocyte ferroptosis in a HIF-2alpha-dependent manner. Cell Prolif 2021;54(11):e13134.
[34] Park S, Baek IJ, Ryu JH, Chun CH, Jin EJ. PPARalpha-ACOT12 axis is responsible for maintaining cartilage homeostasis through modulating de novo lipogenesis. Nat Commun 2022;13(1):3.
[35] Łuczaj W, Gindzienska-Sieskiewicz E, Jarocka-Karpowicz I, Andrisic L, Sierakowski S, Zarkovic N, et al. The onset of lipid peroxidation in rheumatoid arthritis: consequences and monitoring. Free Radic Res 2016;50(3):304–13.
[36] Akasaki Y, Alvarez-Garcia O, Saito M, Carames B, Iwamoto Y, Lotz MK. FoxO transcription factors support oxidative stress resistance in human chondrocytes. Arthritis Rheumatol 2014;66(12):3349–58.
[37] Lee KI, Choi S, Matsuzaki T, Alvarez-Garcia O, Olmer M, Grogan SP, et al. FOXO1 and FOXO3 transcription factors have unique functions in meniscus development

and homeostasis during aging and osteoarthritis. Proc Natl Acad Sci U S A 2020; 117(6):3135–43.
[38] Matsuzaki T, Alvarez-Garcia O, Mokuda S, Nagira K, Olmer M, Gamini R, et al. FoxO transcription factors modulate autophagy and proteoglycan 4 in cartilage homeostasis and osteoarthritis. Sci Transl Med 2018;10(428).
[39] Park E, Chung SW. ROS-mediated autophagy increases intracellular iron levels and ferroptosis by ferritin and transferrin receptor regulation. Cell Death Dis 2019; 10(11):822.
[40] Zhang Z, Guo M, Li Y, Shen M, Kong D, Shao J, et al. RNA-binding protein ZFP36/TTP protects against ferroptosis by regulating autophagy signaling pathway in hepatic stellate cells. Autophagy 2020;16(8):1482–505.
[41] Chang SH, Mori D, Kobayashi H, Mori Y, Nakamoto H, Okada K, et al. Excessive mechanical loading promotes osteoarthritis through the gremlin-1-NF-kappaB pathway. Nat Commun 2019;10(1):1442.
[42] Guo Q, Chen X, Chen J, Zheng G, Xie C, Wu H, et al. STING promotes senescence, apoptosis, and extracellular matrix degradation in osteoarthritis via the NF-kappaB signaling pathway. Cell Death Dis 2021;12(1):13.
[43] Yoon DS, Lee KM, Choi Y, Ko EA, Lee NH, Cho S, et al. TLR4 downregulation by the RNA-binding protein PUM1 alleviates cellular aging and osteoarthritis29. Cell Death Differ; 2022. p. 1364–78.
[44] Collins JA, Arbeeva L, Chubinskaya S, Loeser RF. Articular chondrocytes isolated from the knee and ankle joints of human tissue donors demonstrate similar redox-regulated MAP kinase and Akt signaling. Osteoarthritis Cartilage 2019;27(4): 703–11.
[45] Chen Z, Yang X, Zhou Y, Liang Z, Chen C, Han C, et al. Dehydrocostus lactone attenuates the senescence of nucleus pulposus cells and ameliorates intervertebral disc degeneration via inhibition of STING-TBK1/NF-kappaB and MAPK signaling. Front Pharmacol 2021;12:641098.